OPTIMAL DESIGN OF BALL BEARING RETAINERS USING TAGUCHI METHODS AND BEARING DYNAMIC ANALYSIS

Kazuaki Maniwa[(1)], Takashi Nogi[(1)], Kazuo Natori[(1)] & Shingo Obara[(1)]

[(1)]Japan Aerospace Exploration Agency (JAXA)
Tsukuba Space Center, 2-1-1 Sengen, Tsukuba-shi, Ibaraki-ken 305-8505, JAPAN
Email: maniwa.kazuaki@jaxa.jp

ABSTRACT

The authors developed an optimal design technique for ball bearing retainers, which combines the Taguchi method and a bearing dynamic analysis and takes a mixed lubrication model for retainer-race and retainer-ball contacts into consideration.

It is clarified that retainer stability under bearing rotation can be improved by designing a high signal-to-noise ratio using the present design technique.

The designed retainer with a high signal-to-noise ratio performed well in a bearing rotating test, in which no significantly increased torque and audible noise were observed.

1. INTRODUCTION

Oil-lubricated ball bearings used for space applications such as a gyroscope and reaction wheel are usually operated at relatively high rotational speeds, typically thousands of RPM, and must also rotate with extremely low frictional torque under a vacuum. Therefore, the amount of lubricant oil must be strictly restricted to reduce the viscous friction of oil. A cotton-based phenol retainer impregnated with the lubricant oil has been used to achieve a long operating lifetime in minimally lubricated ball bearings.

During the operation of ball bearings assembled with a cotton-based phenol retainer, retainer instability often leads to problematic increased frictional torque and audible noise. According to the author's experiences, the incidence of retainer instability is greatly affected by the dimensions of guiding clearance and pocket clearances in Fig. 1 and frictional characteristics at their mating surfaces. Therefore, designing the retainer clearances appropriately is vital to prevent retainer instability. However, hardly any design approaches taking the optimization technique into account have been conducted to date, with designers mostly reliant on parametric experiments and lessons learned.

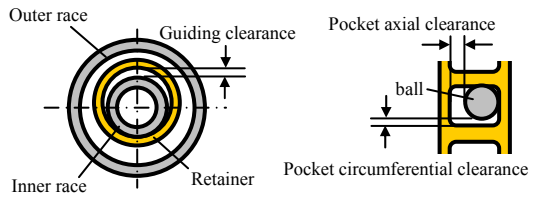

Figure 1. Retainer clearances in case of inner race guiding and rectangular pocket

To clarify the generation mechanism of retainer instability and design the ball bearing retainer numerically, the authors developed a bearing dynamic analysis model, which takes a mixed lubrication model for the retainer-race and retainer-ball contacts into consideration [1], [2]. The retainer design is likely to become more efficient by combining the bearing dynamic analysis with an optimization technique. The objective of this study is to develop an optimal design technique for ball bearing retainers using the parameter design technique in the Taguchi method and bearing dynamic analysis. The Taguchi method is generally thought to be capable of estimating "robustness", which is probably suitable for evaluating retainer stability.

2. BEARING DYNAMIC ANALYSIS

In this analysis, the outer race is assumed to be fixed in space, while the inner race rotates at constant speed. Equations of the motion of balls and retainer are numerically integrated, considering the gravity in 6-degrees of freedom. During ball-race contact, normal load is calculated using the Hertz equation, whereupon traction force and rolling resistance are estimated. For retainer-race and retainer-ball contacts, normal load and friction force are calculated according to the mixed lubrication model, whereby the oil film thickness and surface roughness of the retainer are considered [1], [2]. The normal load and friction force between the retainer and race/ball are expressed as:

$$w = w_f + w_a \tag{1}$$

$$f = f_f + f_a \tag{2}$$

where w and f denote contact load and friction force, respectively and subscripts f and a denote fluid film lubrication and asperity contact, respectively.

'14th European Space Mechanisms & Tribology Symposium – ESMATS 2011'
Constance, Germany, 28–30 September 2011

The numerical analysis conditions are listed in Tab. 1. The targeted bearing is an angular contact ball bearing, with an inner diameter of 10 mm, outer diameter of 26 mm and width of 8 mm respectively. The bearing is assumed to be lubricated with Multiply Alkylated Cyclopentane at a temperature of 40 ºC. A horizontal shaft at 1 G for the bearing attitude is applied to simulate tests, on the premise that the motion of the retainer is prone to fluctuate compared with zero gravity conditions [3].

Table 1. Numerical analysis conditions

Bearing type	Angular contact ball bearing
Bearing size	Inner diameter 10 [mm] Outer diameter 26 [mm] Width 8 [mm]
Number of balls	9
Rotational speed of inner race	5000 [RPM]
Lubricant viscosity	0.096 [Pa·s] : corresponding to the viscosity of Multiply Alkylated Cyclopentane at 40 ºC
Bearing attitude	Horizontal shaft in 1 G
Simulation time	6 [s] (corresponding to 500 revolutions of the inner race)

3. APPLICATION OF THE TAGUCHI METHOD

In the parameter design of the Taguchi method, we identify the system output associated with the design concept and set control factors and noise factors for a robust design. Noise factors result in the output variation of the system used to evaluate robustness.

In this study, the mean of the retainer translational velocity is assumed to be an output in the Taguchi method to evaluate the retainer stability, because the retainer translational velocity is sensitive to whether retainer instability occurs. The retainer translational velocity v is expressed as

$$v = \sqrt{v_x^2 + v_y^2 + v_z^2} \tag{3}$$

where subscript x corresponds to axial direction and subscripts y and z correspond to the radial direction in an inertial coordinate system.

We selected eight parameters as Taguchi method control factors, the factors and levels of which are shown in Tab. 2. The retainer-race and the retainer-ball clearances, the oil film thickness and the surface roughness of the retainer are chosen as control factors. The oil film thickness is usually determined by the initial amount of supplied oil and operating conditions such as rotational speed and preload. In the present design technique, the oil film thickness is selected as a control factor to evaluate its effect on retainer stability. A rectangular pocket shape was selected in this study, because a rectangular pocket shape was presumed to be more advantageous in terms of stabilizing retainer behavior than the circular pocket shape already reported in [1].

As shown in Tab. 3, slight changes in the oil film thicknesses were given to the guiding land and the pockets as noise factors. For example, the state where both oil film thicknesses decrease to 0.9 times the nominal level corresponds to N1. To investigate eight kinds of control factors, an orthogonal array L_{18} shown in Tab. 4 was selected. Namely, a total of 72 (= 18 × 4 noise factors) cases of numerical analyses were conducted, whereupon the signal-to-noise (S/N) ratio and sensitivity in the case of nominal-the-best

Table 2. Control factors

Control factors	Level		
	1	2	3
A Preload	S	L	-
B Guiding clearance	S	M	L
C Pocket axial clearance	S	M	L
D Pocket circumferential clearance	S	M	L
E Guiding land oil film thickness	S	M	L
F Pocket oil film thickness	S	M	L
G Guiding land surface roughness	S	M	L
H Pocket surface roughness	S	M	L

S: small, M: middle, L: large

Table 3. Noise factors

Noise factors	N1	N2	N3	N4
E Guiding land oil film thickness	0.9	0.9	1.1	1.1
F Pocket oil film thickness	0.9	1.1	0.9	1.1

Table 4. Orthogonal array L_{18}

No.	A	B	C	D	E	F	G	H
1	1	1	1	1	1	1	1	1
2	1	1	2	2	2	2	2	2
3	1	1	3	3	3	3	3	3
4	1	2	1	1	2	2	3	3
5	1	2	2	2	3	3	1	1
6	1	2	3	3	1	1	2	2
7	1	3	1	2	1	3	2	3
8	1	3	2	3	2	1	3	1
9	1	3	3	1	3	2	1	2
10	2	1	1	3	3	2	2	1
11	2	1	2	1	1	3	3	2
12	2	1	3	2	2	1	1	3
13	2	2	1	2	3	1	3	2
14	2	2	2	3	1	2	1	3
15	2	2	3	1	2	3	2	1
16	2	3	1	3	2	3	1	2
17	2	3	2	1	3	1	2	3
18	2	3	3	2	1	2	3	1

characteristic were calculated from the numerical analysis results of 72 cases. The interpretations of the S/N ratio and sensitivity are as follows:

(1) The higher the S/N ratio, the less the noise factors influence the retainer translational velocity, namely the greater the "robustness".

(2) The lower the sensitivity, the smaller the retainer translational velocity.

4. NUMERICAL ANALYSIS RESULTS

Fig. 2 shows the numerical analysis results of the mean retainer translational velocity. The numbers in the horizontal axis correspond to each analysis condition in the orthogonal array L_{18}. The high retainer translational velocity at number 10 is due to the retainer instability, whereas the retainer translational velocity at N2 of number 15 differs significantly from other noise conditions, namely poor "robustness".

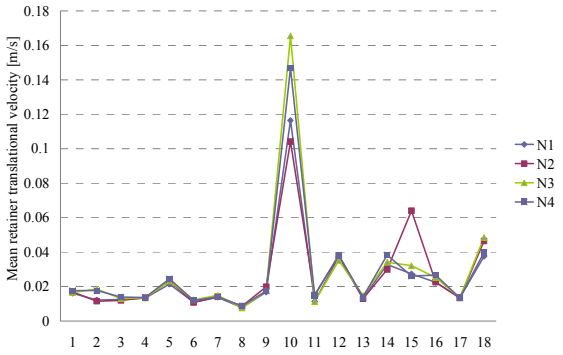

Figure 2. Numerical analysis results of the mean retainer translational velocity

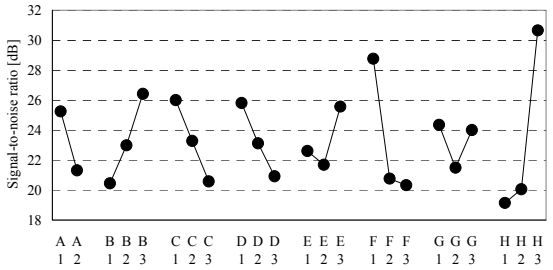

Figure 3. Graphs of the factorial effects of the S/N ratio

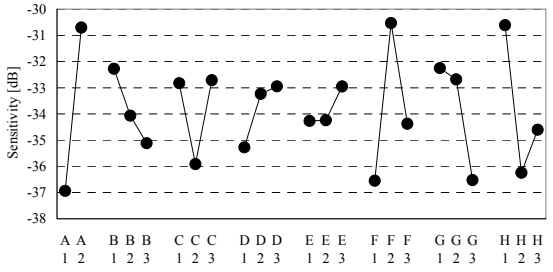

Figure 4. Graphs of the factorial effects of the sensitivity

Figs. 3 and 4 show graphs of the factorial effects of the S/N ratio and the sensitivity, respectively. From Fig. 3, the parameter that changes the S/N ratio in particular is the pocket oil film thickness (F) and the pocket surface roughness (H). The S/N ratio rises when the guiding clearance (B) increases and both pocket clearances (C and D) decline. Conversely, as shown in Fig. 4, the parameter that particularly changes the sensitivity is the preload (A), the pocket oil film thickness (F) and the pocket surface roughness (H). Basically, the sensitivity can remain small when the S/N ratio is designed to be high.

Tab. 4 shows the levels of each control factor with the S/N ratio under optimal and worst conditions. In addition, Tab. 5 shows results of the prediction and confirmation of the gains. Gain here refers to the reference value, whereby the optimal condition shows the extent to which the S/N ratio and sensitivity have improved relative to the related condition. The related condition is assumed to be the worst condition of the S/N ratio in the present design technique. In general, if the results of confirmation correspond to the prediction in the gain, the analysis results can be implemented with high reliability, namely "good repeatability". As for the S/N ratio gain, the prediction and confirmation differ by 9.8 dB from Tab. 5. The reason why a difference between the prediction and confirmation in the S/N ratio is generated can be explained by (1) interaction between the retainer clearances and the oil film thicknesses, and (2) the occurrence of retainer instability.

Table 4. Optimal and worst conditions of the S/N ratio

	A	B	C	D	E	F	G	H
Optimal condition	1	3 1		1	3	1 1 3		
Worst condition	2	1 3		3	2	3 2 1		

Table 5. The prediction and confirmation of the gain

	Prediction		Confirmation	
	S/N ratio	Sensitivity	S/N ratio	Sensitivity
Optimal condition	49.85	-39.78	36.47	-32.54
Worst condition	2.90	-23.81	-0.66	-20.64
Gain	46.95	-15.97	37.13	-11.90

Figs. 5 and 6 show the numerical analysis results of the retainer translational velocity and loci of the retainer center under optimal and worst conditions respectively. Under the optimal condition, the retainer translational velocity is low and stable as shown in Fig. 5 (a), and the retainer shows pendulum-like motion at the bottom of the clearance circle according to the gravity in Fig. 6 (a). Conversely, under the worst condition, the retainer translational velocity is high and unstable as shown in

Fig. 5 (b), and the retainer shows whirling motion in Fig. 6 (b), which is thought to indicate retainer instability. Fig. 7 shows the numerical analysis results of the frictional torque under optimal and worst conditions respectively. The increased fluctuation in frictional torque in Fig. 7 (b) is thought to be attributable to the increased contact load applied to the retainer-race and retainer-ball, induced by retainer instability. Although insufficient repeatability is obtained (variation of 9.8 dB in the S/N ratio), the numerical analysis results in Figs. 5-7 are judged to indicate that the present design technique is effective in stabilizing the retainer behavior and improving the bearing frictional torque.

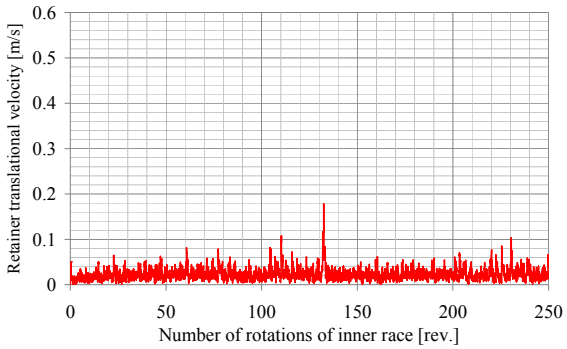

(a) Optimal condition

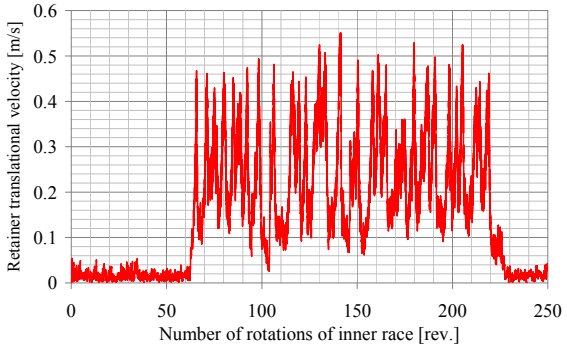

(b) Worst condition

Figure 5. Numerical analysis results of the retainer translational velocity

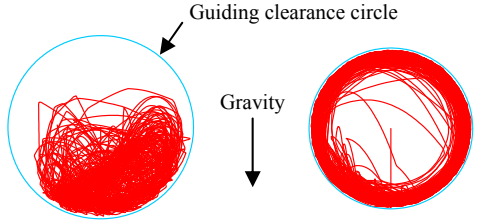

(a) Optimal condition *(b) Worst condition*

Figure 6. Numerical analysis results of loci of the retainer center

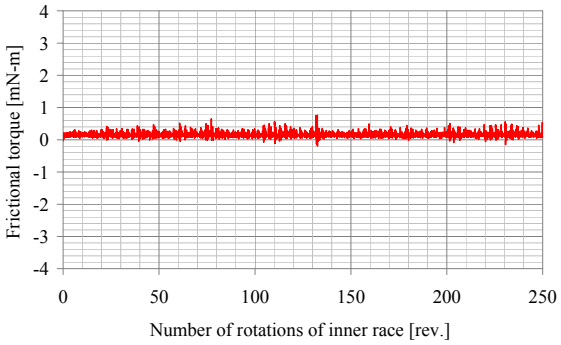

(a) Optimal condition

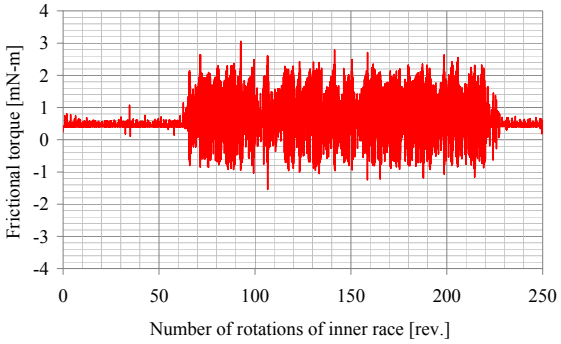

(b) Worst condition

Figure 7. Numerical analysis results of the frictional torque

5. BEARING ROTATING TEST

To examine the stability of the designed retainer, a bearing rotating test was conducted.

5.1. Test Method

The test bearing is an angular contact ball bearing with inner diameter of 10 mm, outer diameter of 26 mm and width of 8 mm, of equivalent size to that used for the numerical analysis. Two kinds of cotton-based phenol retainers were prepared: (1) type A, the pocket circumferential clearance of which is slightly smaller than level 1 in Tab. 2, (2) type B, the pocket circumferential clearance of which is slightly larger than level 3 in Tab. 2. The guiding and pocket axial clearances in types A and B are set to be level 2. Moreover, since retainer types A and B were fabricated and lubricated under equivalent conditions, their surface roughness and oil film thickness were considered almost similar. It is presumed from Fig. 3 that the S/N ratio of retainer type A is higher than that of retainer type B.

Fig. 8 shows a photograph and schematic diagram of the bearing tester. A pair of test bearings set up in a vacuum chamber is rotated by the motor through the magnetic coupling. An axial load of about 29 N is applied to the test bearings by position preloading. The

frictional torque and temperature of the test bearings under rotation are measured with the load cell and thermocouple, respectively. By circulating an anti-freeze solution through the cooling shroud, the test bearings can be cooled to about -4 ºC. Tab. 6 shows the bearing rotating test conditions. The bearing rotating tests were conducted at a rotational speed of 5000 RPM in three different environments. The low temperature environment (-4 ºC) was selected as the test environment, because the high lubricant viscosity meant retainer instability was considered likely to occur. During the initial stage of the test, the bearings were operated at rotational speeds of 1000, 2000, 3000 and 4000 RPM every 10 min, whereupon the bearing rotating test at 5000 RPM was started.

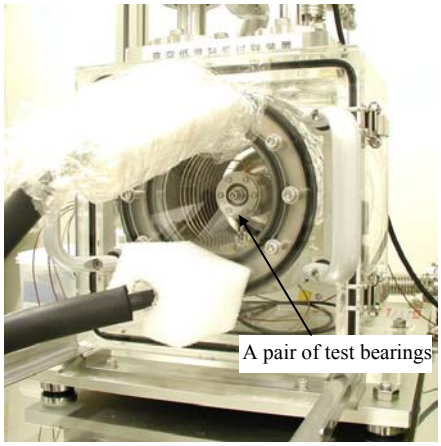

(a) Photograph

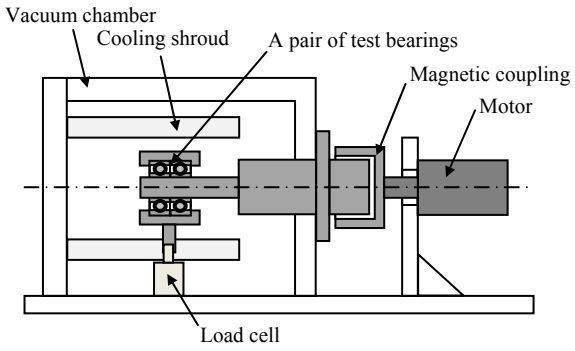

(b) Schematic diagram

Figure 8. Bearing tester

Table 6. Bearing rotating test conditions

Rotational speed of the inner race	5000 [RPM]
Lubricating oil	Multiply Alkylated Cyclopentane (formulated)
Environment (pressure, temperature, test duration)	(a) Atmospheric pressure (dry nitrogen gas), room temperature (22 ºC), 24 hr (b) Atmospheric pressure (dry nitrogen gas), low temperature (-4 ºC), 24 hr (c) Vacuum pressure (less than 100 Pa), room temperature (22 ºC), over 90 hr

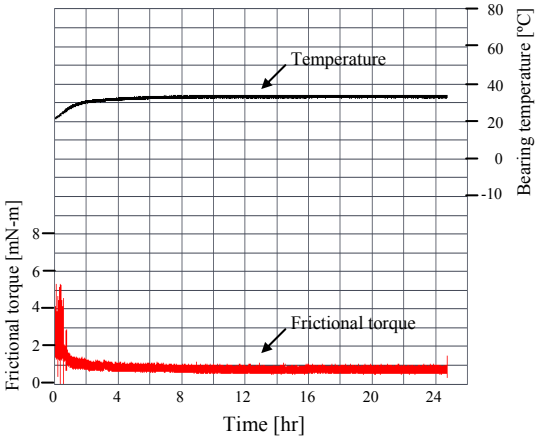

(a) Atmospheric pressure, room temperature

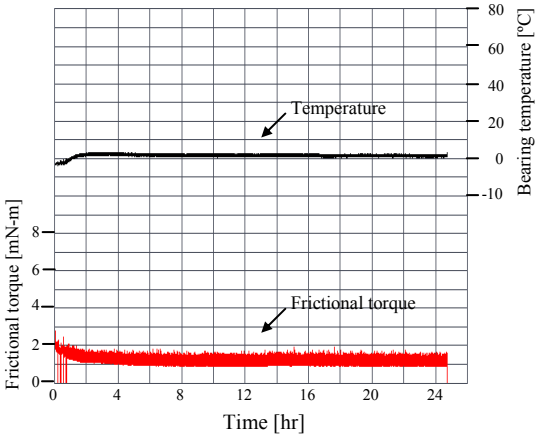

(b) Atmospheric pressure, low temperature

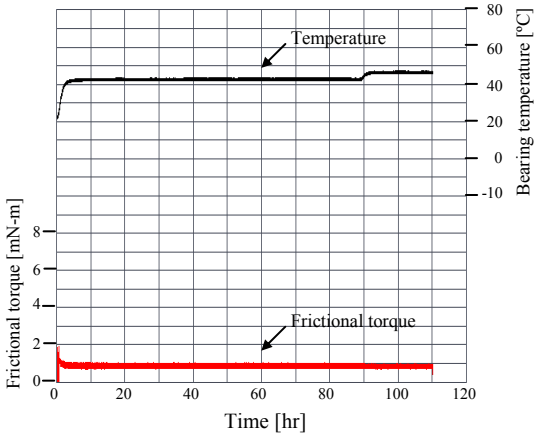

(c) Vacuum pressure, room temperature

Figure. 9 Results of bearing rotating test for retainer type A with high S/N ratio

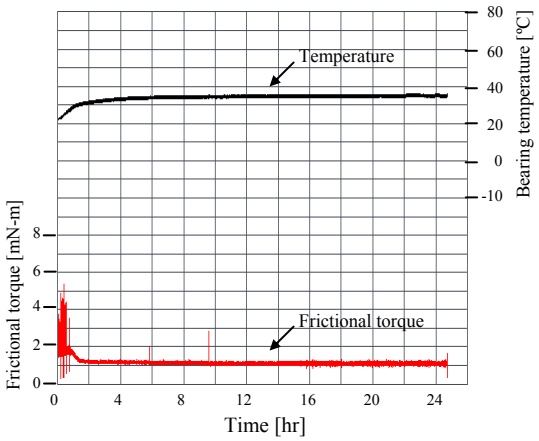

(a) Atmospheric pressure, room temperature

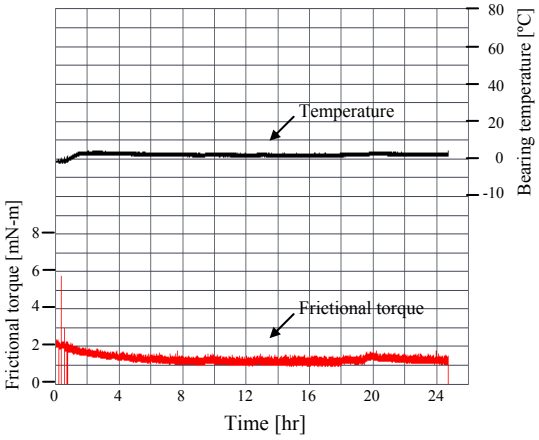

(b) Atmospheric pressure, low temperature

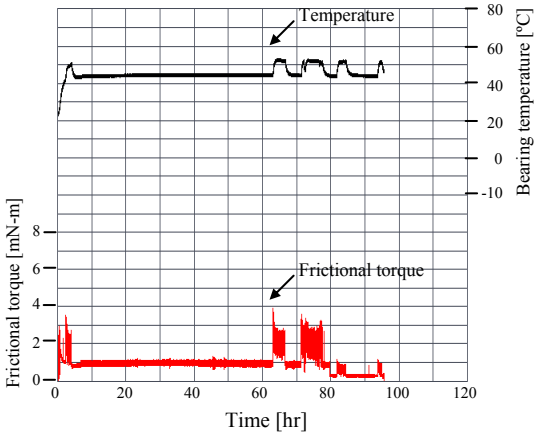

(c) Vacuum pressure, room temperature

Figure. 10 Results of bearing rotating test for retainer type B with low S/N ratio

5.2. Test Results

Figs. 9 and 10 show the results of bearing rotating tests for retainer types A and B, respectively. The horizontal axis represents time, whereas the vertical axis represents the frictional torque and temperature of the test bearings. For the retainer type A in Fig. 9, the frictional torque is low and stable in any environment. For the retainer type B in Fig. 10, the frictional torque appears almost completely low and stable in environments (a) and (b), similar to the retainer type A. However, the frictional torque and temperature rise several times in the environment (c). Audible noises were also generated during the torque fluctuation; phenomena which are considered to indicate retainer instability.

It was confirmed that the retainer designed using the present technique with a high S/N ratio performed well in the bearing rotating test, hence the present design technique is considered useful for determining the stable dynamic behavior of the ball bearing retainer.

6. CONCLUSIONS

The optimal design technique for a ball bearing retainer was developed combining bearing dynamic analysis and the parameter design technique in the Taguchi method. In the present design technique, the retainer translational velocity is selected as the output, whereas the clearances, oil film thickness and surface roughness of the retainer are the selected control factors. To evaluate "robustness", noise factors are assigned by varying the oil film thickness slightly in numerical analysis.

Cotton-based phenol retainers for angular contact ball bearings with a 10 mm bore were designed using the present technique. For two kinds of designed retainers, with high and low S/N ratios, bearing rotating tests under atmospheric pressure and a vacuum were respectively conducted to confirm their stability. Consequently, the retainer with a high S/N ratio performed well. This result indicates that the present design technique is useful for designing high stability retainers of ball bearings.

7. REFERENCES

1. Nogi, T., Maniwa, K. & Obara, S. (2008). Dynamic Analysis of Minimally Lubricated Ball Bearings for Space Applications. In *Proc. STLE/ASME International Joint Tribology Conference*, IJTC2008-71154, Miami, Florida USA, pp 433-436.
2. Nogi, T., Maniwa, K. & Obara, S. (2009). Numerical Analysis of Cage Instability in Minimally Lubricated Ball Bearings. *In Proc. World Tribology Congress 2009*, Kyoto, Japan, 596.
3. Obara, S. & Sato, M. (2001). Numerical Investigation of Influence of Gravity on the Performance of Ball Bearings Assembled in a Space Device. In *Abstracts of papers 2nd World Tribology Congress*, Vienna, Austria, 607.